Biophysical Chemistry 20 (1984) 249–259
Elsevier

BPC 00881

SIMULATIONS OF FREQUENCY-DEPENDENT PHOTOACOUSTIC MAGNITUDE SIGNALS AND THEIR IMPLICATIONS FOR BACTERIORHODOPSIN PHOTOCYCLE ENERGETICS

Jane LEGRANGE [a,*], S. Roy CAPLAN [a,**] and David CAHEN [b]

[a] *Department of Membrane Research and* [b] *Department of Structural Chemistry, Weizmann Institute of Science, Rehovot 76100, Israel*

Received 26th February 1984
Accepted 17th May 1984

Key words: *Photoacoustic spectroscopy; Photocalorimetry; Kinetics; Energetics; Bacteriorhodopsin; Purple membrane; (H. halobium)*

The modulation frequency dependence of photoacoustic signals obtained from photoactive samples can provide information on the time-dependent enthalpy changes occurring during the light-induced process. The experimental requirements for this type of calorimetry, and the interpretation of the results, are critically examined with reference to the light-driven proton pump bacteriorhodopsin. For a three-step unbranched model of the bacteriorhodopsin photocycle we derive an expression for the photoacoustic magnitude signal as a function of frequency. Simulations are performed for various values of the rate constants and energetic changes. It is shown that the net heat uptake during a low, final step postulated by some workers should be reflected in the photoacoustic magnitude frequency spectrum, giving rise to a characteristic maximum. However, this effect, which has been observed experimentally, may also be produced by a fast, strongly endothermic step occurring earlier. The precise chronology of an endothermic transition cannot be resolved unambiguously by magnitude measurements alone, although they are free from assumptions regarding difficult-to-measure phase relationships. Hence, the published photoacoustic observations showing the effect are consistent with a cyclic sequence of events in which the bacteriorhodopsin system first undergoes an increase of entropy, followed by a decrease on returning to the initial state, as well as the reverse. It is argued that the molecular disorder-order sequence is more probable.

1. Introduction

Photoacoustic spectroscopy is a modulation technique in which light pulses absorbed by a sample are converted to acoustic pulses via the production of heat by the sample. The pressure wave is monitored at the frequency of excitation by a microphone or piezoelectric device, amplified, and recorded by a lock-in amplifier [1].

Most applications of this technique have been directed toward the investigation of optical absorption characteristics of a sample using wavelength spectra, assuming the photoacoustic signal to be proportional to light absorption. In recent years our group has attempted to utilize the photoacoustic technique for time-dependent studies of the energetics of photosynthetic systems [2]. We have claimed, for example, that the photoacoustic frequency spectra of bacteriorhodopsin (bR) may be interpreted in terms of the change in sample enthalpy as a function of time after photon absorption [3].

The protein bR functions as a light-driven proton pump in the well-known purple membrane of *Halobacterium halobium* [4]. After light preadaptation, the chromophore prior to excitation is all-*trans*-retinal bound to a lysine moiety via a protonated Schiff base link, and its ground-state absorption peaks at 570 nm. Upon absorption of a photon, the protein undergoes a cycle commencing

---

* Present address: Department of Physics, Princeton University, Princeton, NJ 08544, U.S.A.

** To whom reprint requests should be addressed.

0301-4622/84/$03.00

with a fast photoreaction (picosecond time scale), followed by a much slower return cascade of thermally excited intermediates and possibly intermediates arising through charge separation (micro- to millisecond time scales) during which protons are pumped across the membrane from the cytoplasmic to the outer side of the cell. The resulting electrochemical potential gradient is used as an energy source in the synthesis of ATP [5]. Detailed thermodynamic information on this simple photosynthetic system would greatly enhance our understanding of the mechanisms of energy transduction in biology. Theoretical descriptions of the light-driven proton transport [6,7] make predictions concerning the energetics of bR as a proton pump. Reliable measurements of the energy dissipated as a function of time could provide a key to the correct model.

Since traditional calorimetric methods depend on the sample being in thermal equilibrium, they are not appropriate for studies of the energy changes taking place during a transduction process. Here we present numerical simulations of the frequency dependence of that part of the photoacoustic vector amplitude which is due to chemical changes. The latter are assumed to occur during a simple, three-step, photoinduced process. In this way the effects of the separation in time between the steps and of the presence of an endothermic step can be followed. It is shown that although there is a characteristic frequency spectrum which is always associated with the occurrence of an endothermic step, the magnitude and chronology of the step cannot be determined unambiguously from measurements of the vector amplitude (i.e. the magnitude signal) alone. Furthermore, the occurrence of an endothermic step cannot be excluded when this spectral characteristic is absent In particular, the observed endothermic step in the bR photocycle need not necessarily reflect the final event, as was assumed to be the case [3].

2. Theoretical

The photoacoustic effect is based on the conversion of a modulated light signal to a modulated acoustic signal reflecting heat released by the optically excited sample. A liquid or solid specimen in a sealed cell is excited by chopped light. The periodic heat flow produced by non-radiative decay processes in the sample heats a thin layer of air at the sample surface. The thermal modulation of this gas layer causes it to act as a piston, and an acoustic wave is created in the cell.

Photoacoustic calorimetry is not an equilibrium measurement; indeed, the thickness of sample contributing to the measured temperature oscillation varies with frequency. The relative magnitudes of the optical absorption length, thermal diffusion length and sample thickness determine the frequency dependence of the signal.

Rosencwaig and Gersho [1] formulated a one-dimensional model for heat flow in the photoacoustic cell. The solution to the thermal diffusion equation,

$$\frac{\partial^2 T}{\partial x^2} = \frac{1}{\alpha_s}\frac{\partial T}{\partial t} - A\exp(\beta x)[1+\exp(i\omega t)] \qquad (1)$$

yields the temperature oscillation in the sample as a function of time (t) and distance (x) from the sample surface (T, temperature; α_s, thermal diffusivity of the sample in cm^2 s^{-1}; β, absorption coefficient in cm^{-1}). The coefficient A is given by

$$A = \beta\eta I_0/2k_s \qquad (2)$$

where η is the 'efficiency' at which the absorbed light is converted to heat, I_0 the light intensity at the sample surface (in J cm^{-2} s^{-1}) and k_s the thermal conductivity of the sample (in J cm^{-1} s^{-1} °C^{-1}). The forcing function f for the differential equation is

$$f = A\exp(\beta x)(1+\cos\omega t) \qquad (3)$$

This describes the density of heat produced at time t at a depth x due to the light absorbed. If the sample is photoactive and forms intermediates whose lifetimes are on the time scale of the period of excitation, the forcing function becomes

$$f = A(\omega)\exp(\beta x)[1+\cos(\omega t+\psi)] \qquad (4)$$

i.e., it is phase-shifted by ψ. In addition, its amplitude is reduced by a coefficient, $B(\omega)$, containing terms dependent on the kinetic and energetic behavior of the sample. $B(\omega)$ multiplies ηI_0, as it represents the frequency-dependent fraction of the absorbed radiation that is converted to heat during the photoinduced process. The heat measured by the photoacoustic method is released in the decay of photochemical intermediates. If those intermediates have lifetimes much shorter than the period of oscillation, the heat production is not reduced by the energy stored in the intermediates. There is effectively no delay time between the absorption of light and the release of heat energy, and hence no phase shift in the forcing function (eq. 3). Rosencwaig and Gersho solve eq. 1 for the sample using analogous equations for the gas above the sample surface and the backing of the cell, and apply the appropriate boundary conditions for the gas/sample and sample/cell interfaces. Their solution holds when all of the intermediates have decayed. If less heat is produced instantaneously because of energy storage in photochemical intermediates, the amplitude of the solution is reduced by the kinetic-energetic coefficient, $B(\omega)$.

Malkin and Cahen [2] derive solutions for the sine and cosine components of the population of intermediates for two- and three-step consecutive transitions. The amplitude of these components (the square root of the sum of the squares of the sine and cosine parts) gives the coefficient of the driving force in the thermal diffusion equation. The solution to eq. 1, the expression for the pressure wave, Γ, created by the heat released from the sample, is a complex function depending on the thermal properties and dimensions of the sample, the optical absorption β, and η. It may be expressed in terms of amplitude and phase ($\Gamma = \gamma e^{-i\psi}$) or in terms of components ($\Gamma = \Gamma_1 + i\Gamma_2$). The amplitude is the most convenient quantity to measure and analyze: it always contains the factor ηI_0, or in the case of a photochemically active sample, $B(\omega)\eta I_0$. The phase shift is much more difficult to interpret and measure. Experimentally there are thermodynamic and instrumental factors which contribute to ψ, and changes in ψ as a function of frequency are less readily determined than those in γ.

Garty et al. [3] introduced the idea of using the ratio of photoacoustic signal amplitudes for an active sample, in our case purple membrane, and for an inactive dye. (Here, inactive means that all photochemical intermediates decay much faster than the period of oscillation.) If such a 'fast dye' is matched to a biological sample in terms of its thermodynamic and optical parameters, the ratio of their magnitude frequency spectra yields $B(\omega)$, as all other factors cancel. This normalized spectrum gives the frequency dependence of the kinetics and the fraction of the absorbed energy dissipated as heat, and strictly speaking may only be obtained from measurements of amplitude as a function of frequency. Since the individual components of Γ are characterized, in general, by different phase shifts for photoactive and photoinactive samples, a ratio cannot be established between the sine or cosine components alone unless the assumption is made that both the photoactive and the photoinactive samples exhibit not only small but identical phase shifts with respect to a reference signal at very low frequencies. This assumption is very difficult to test, and depends, inter alia, on identical geometries for the photoactive and photoinactive samples. On the other hand, measurements of γ and ψ may in principle be used to correct the observed values of the components and hence remove the assumption, providing reliable values for ψ can be obtained (D. Cahen, unpublished result). It should be mentioned that this experimental difficulty does not exist if the sample can serve as its own photoinactive reference. This is the case for photosynthetic samples where modulated photoactivity can be made to vanish by adding additional strong, nonmodulated, excitation, and for photovoltaic systems where photoactivity can be made zero by performing measurements under conditions of infinite resistance (open circuit) [2].

It is worth noting that in our laboratory the photoinactive reference sample is made by first photobleaching purple membrane fragments using hydroxylamine, as described by Oesterhelt and Stoeckenius [8]. Several microliters of waterproof drawing ink are then added to a suspension of bleached fragments and the absorbance of the ink-membrane suspension is adjusted to match that of the photoactive sample [3,9]. The lifetime of the excited state of the dye is very short on the time scale of the photoacoustic chopping frequencies, and we can assume that all of the absorbed light energy is released as heat. It is important that the dye be tightly bound to membrane fragments in a suspension physically like the purple membrane suspension, so that thermodynamic parameters such as thermal conductivities and heat capacities are matched (as well as the optical absorption length). The thermal boundary resistance between membrane fragments and surrounding medium affects the overall signal, so the use of a pure dye or an incompletely bound dye as the reference is inadequate. We find that on centrifuging the reference suspension the pellet of membrane fragments contains all the ink, confirming that essentially complete binding has occurred.

The fundamental equation for the photoacoustic calorimetry of a photochemical process is

$$B(\omega, \lambda) = (\rho/\rho_{\mathrm{ref}})(\omega, \lambda) = 1 - \frac{\sum_{i=1}^{n(\omega)} \phi_i(\lambda)\Delta U_i}{Nhc/\lambda} \tag{5}$$

where ρ and ρ_{ref} are, respectively, the photoacoustic magnitude signals from sample and photoinactive reference (as described above), λ the wavelength of measurement, and ϕ_i and ΔU_i the quantum yield and change in internal energy (per mol product) for the i-th photochemical reaction [2]. The primary (fastest) step is denoted here by $i = 1$, while the n-th step is the slowest that still contributes to the measured signal at a given frequency ω. N, h, and c have their usual meanings as Avogadro's number, Planck's constant, and the speed of light in vacuo. Eq. 5 indicates that the fractional dissipation of the incident light energy as heat, which is measured by the magnitude signal ratio, is decreased by the energy storage associated with intermediates whose decay times are long in comparison with the period of illumination. In general, taking into account compositional changes, we can write the Gibbs equation for any change in internal energy as follows:

$$\mathrm{d}U = T\mathrm{d}S - p\mathrm{d}V + \sum_j \mu_j \mathrm{d}n_j \tag{6}$$

where S, p, and V represent entropy, pressure, and volume, respectively, and μ_j and n_j are the chemical potential and number of moles of the j-th species. For all reactions other than those which involve photochemistry directly, the suspension of purple membrane fragments in the photoacoustic cell may be considered a closed system in the usual thermodynamic sense. Hence, the heat exchanged with the gas phase blanketing the suspension is well-defined for these reactions and given by the first law:

$$\mathrm{d}U = \mathrm{d}Q - \mathrm{d}W = \mathrm{d}Q - (\mathrm{d}W' + p\mathrm{d}V) \tag{7}$$

In the above equations $\mathrm{d}Q$ represents heat absorbed and $\mathrm{d}W$ work done by the system; $\mathrm{d}W'$ is 'useful work' other than that done by expansion against the gas phase. From eqs. 6 and 7

$$\mathrm{d}Q = T\mathrm{d}S + \sum_j \mu_j \mathrm{d}n_j + \mathrm{d}W' \tag{8}$$

The enthalpy change of the system, $\mathrm{d}H$, is given by

$$\mathrm{d}H = T\mathrm{d}S - V\mathrm{d}p + \sum_j \mu_j \mathrm{d}n_j \tag{9}$$

The pressure changes which result from the generation of a sound wave in the gas phase are only of the order of 1 μbar, consequently the pressure term in eq. 9 may be regarded as negligible. Therefore, from eqs. 8 and 9

$$\mathrm{d}H = \mathrm{d}Q - \mathrm{d}W' \tag{10}$$

For a suspension of randomly oriented purple membrane fragments no possibility exists of extracting useful work. Hence, the term $\mathrm{d}W'$ in eq. 10 may also be neglected, and our measurements reflect the enthalpy changes of the suspension. These represent a macroscopic average over all of the bR molecules, including those that did not absorb a photon. Among those excited, there is a distribution among the possible states of the photocycle which shifts with the period of illumination. Although individual molecules are not necessarily in thermal equilibrium, the ensemble is characterized by a steady-state population distribution and an average enthalpy for that distribution. As the chopping frequency is varied, we sample the average heat dissipated or enthalpy change for a different time 'window' of the photocycle.

3. Simulations of ratio frequency spectra

Explicit expressions for the dimensionless quantity $B(\omega)$ may be derived from the differential equations for decay of reactants in a multistep photochemical process corresponding to a given λ. As mentioned above, the sine and cosine components of the number of moles of intermediates have been derived as functions of frequency for several models; these solutions can be used to calculate the rate of heat dissipation [2]. Values of $B(\omega)$ are then readily computed by taking the vector sum of the frequency-dependent terms in the amplitudes of the 'in-phase' and 'quadrature' components (i.e., the coefficients of the sine and cosine terms, respectively). This procedure is illustrated for the simplified three-step unbranched model of the bR photocycle depicted in fig. 1. (Since we are discussing a suspension of fragments, we do not need to specify at which stage protons are taken up or released. However, one may obviously identify the model transitions A → B, B → C with the photocycle transitions bR → K, K → M, respectively.) This model essentially corresponds to model III of ref. 2, the result of which, for the rate of heat production per unit volume, $\dot{Q}$, can be written as follows (noting that for modulated light the absorbed intensity has the form $I = I_d + I_a \sin \omega t$):

$$\dot{Q} = \eta I_a N h\nu \left[\left\{ \frac{1}{\eta} - 1 + \frac{E_1 k_1^2}{(k_1^2 + \omega^2)} + \frac{E_2 k_1 k_2 (k_1 k_2 - \omega^2)}{(k_1^2 + \omega^2)(k_2^2 + \omega^2)} \right\} \sin \omega t - \left\{ \frac{E_1 k_1 \omega}{(k_1^2 + \omega^2)} + \frac{E_2 k_1 k_2 (k_1 + k_2)\omega}{(k_1^2 + \omega^2)(k_2^2 + \omega^2)} \right\} \times \cos \omega t \right] \qquad (11)$$

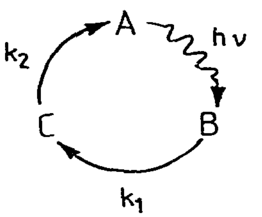

Fig. 1. Simplified three-step model of the bacteriorhodopsin photocycle. B and C are transient species which undergo thermal decay back to the ground state A. Steps A → B, B → C and C → A are in the picosecond, microsecond-millisecond and millisecond time domains, respectively.

Here constant volume is assumed [3], I_a is in E cm^{-3} s^{-1}, $\nu = c/\lambda$, $\eta = \phi(\Delta U_1 + \Delta U_2)/Nh\nu$, and E_1 and E_2 are relative internal energy changes defined by

$$E_1 = \Delta U_1/(\Delta U_1 + \Delta U_2) \qquad E_2 = \Delta U_2/(\Delta U_1 + \Delta U_2) \qquad (12)$$

where ΔU_1 and ΔU_2 are the internal energy changes corresponding to the thermal transitions B → C and C → A, respectively. Hence, by definition,

$$E_1 + E_2 = 1 \qquad (13)$$

Clearly E_1 and E_2 also represent relative enthalpy changes under our conditions. Since the overall reaction B → A is exothermic, a negative value for either E_1 or E_2 indicates that the corresponding step must be endothermic. The vector addition gives the following result for $B(\omega)$:

$$B(\omega) = \frac{k_1 (k_2^2 + \omega^2 E_1^2)^{1/2}}{(k_1^2 + \omega^2)^{1/2} (k_2^2 + \omega^2)^{1/2}} \qquad (14)$$

The limiting case $E_1 = 1$ corresponds in effect to a two-step photocycle, and eq. 14 then reduces to

$$B(\omega) = \frac{k_1}{(k_1^2 + \omega^2)^{1/2}} \qquad (E_1 = 1) \qquad (15)$$

Eq. 15 can also be obtained directly from model I of ref. 2. If we let ω go to 0 in eqs. 14 and 15, $B(\omega)$ tends to 1 as expected, since after relatively long times the intermediates will have decayed. On the other hand, as ω tends to infinity $B(\omega)$ tends to zero, since on this time scale decay of the intermediates is infinitely slow. It is readily seen that whereas $B(\omega)$ can never exceed 1 in the two-step case, it can exceed 1 (and hence pass through a maximum) in the three-step case, but only if $E_1^2 > 1$, i.e, if $E_1 > 1$ or < -1. In either event one step is endothermic. The endothermic transition cannot be identified simply by inspection of the experimental curve, but it is clear that in absolute magnitude the negative enthalpy change involved will be smaller if it is attributable to the final step of the photocycle, which in this model is the slowest step.

It is illuminating to consider two limiting cases, both of which are based on the condition that the rate constants differ greatly in magnitude. The following results are readily obtained from eq. 14:

(a) $k_2 \ll k_1$, $k_2 \ll \omega$

In this frequency range the curve $B(\omega)$ vs. ω passes through an inflection point when $\omega = k_1/\sqrt{2}$. If there is an intermediate frequency range for which the condition $\omega \ll k_1$ holds as well, the curve will plateau at $B(\omega) = E_1$.

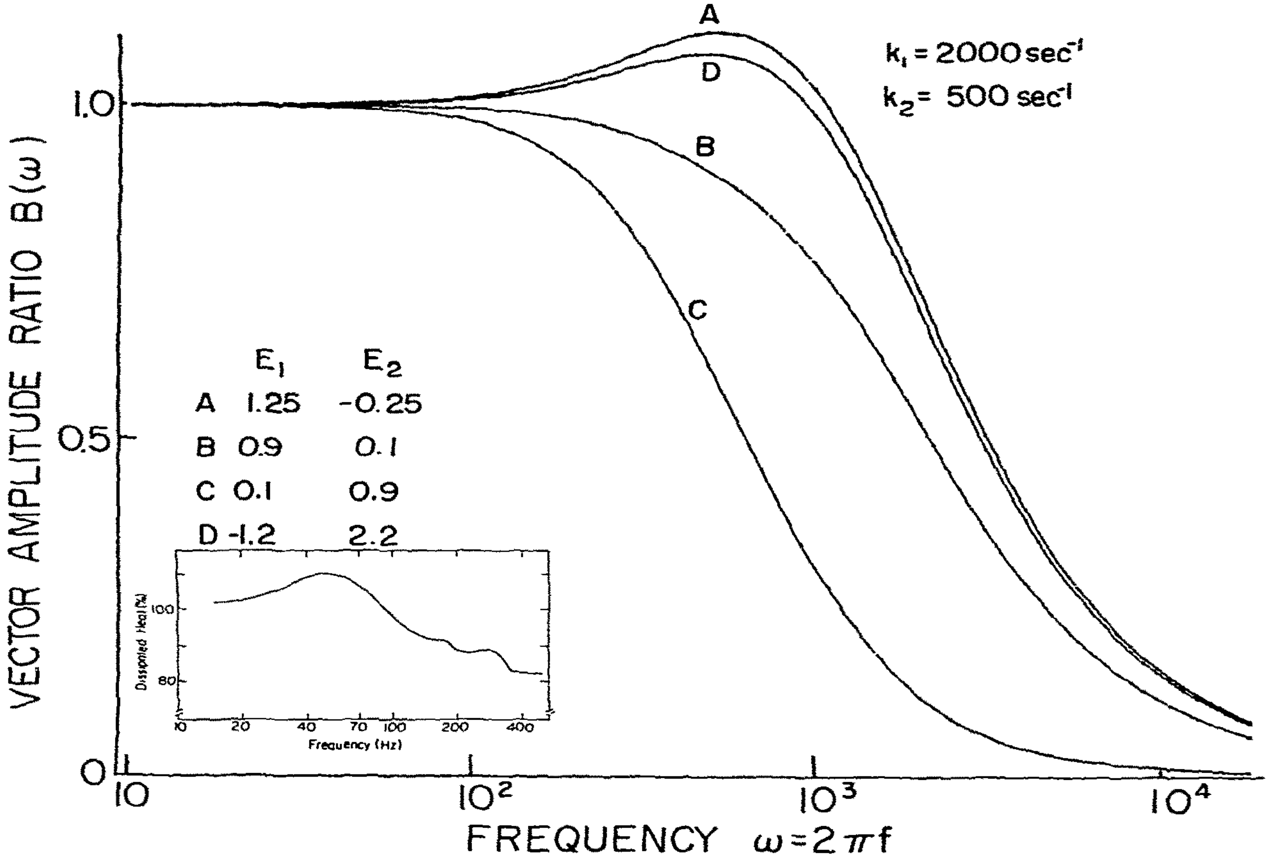

Fig. 2. Simulations of $B(\omega)$ for the model of fig. 1 with $k_1/k_2 = 4$; rate constants and relative internal energy changes as indicated. Curves A and D each show a maximum due to an endothermic step. Curve B shows the simulation for a highly exothermic fast transition. Curve C represents a highly exothermic slow transition. However, the sign of E_1 may in all cases be reversed, producing a corresponding change in the value of E_2, without altering the curve (see text). (Inset) Normalized frequency spectrum for purple membrane fragments buffered at pH 7.0. (The reference is a preparation of bleached membrane fragments treated with black ink.) Curve taken from the data of Garty et al. [3].

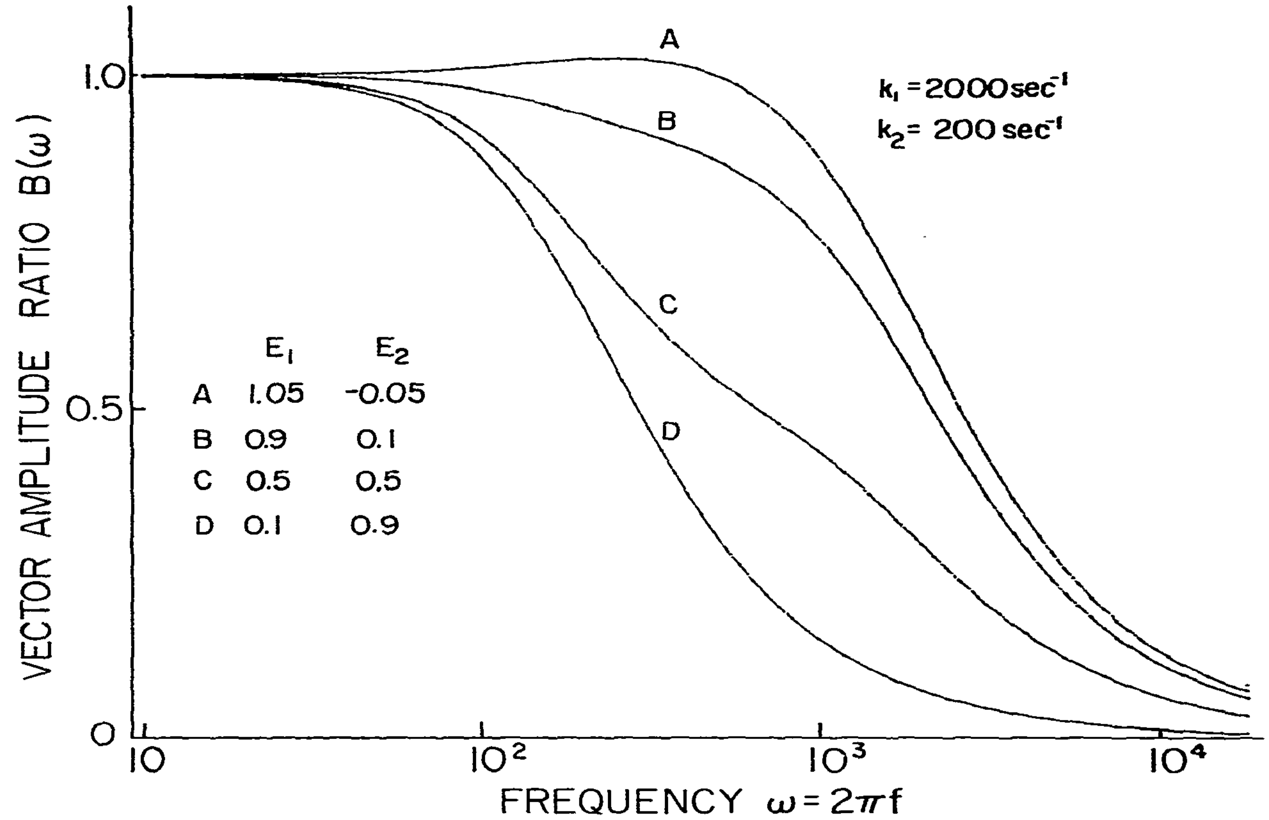

Fig. 3. Simulations of $B(\omega)$ for the model of fig. 1 with $k_1/k_2 = 10$, showing the effect of a slightly endothermic slow transition. Curve C indicates that, with the given rate constants, resolution of the two processes can be most readily obtained if equal dissipation occurs in the decay of the two intermediates.

(b) $k_2 \ll k_1$, $\omega \ll k_1$, $E_1^2 \ll 1$

In this frequency range (providing that E_1^2 is sufficiently small) the curve $B(\omega)$ vs. ω passes through an inflection point when $\omega = k_2/\sqrt{2}$.

These characteristics as well as the general properties of the function $B(\omega)$ are apparent in the simulations shown in figs. 2–4, which were performed with an Apple II Plus microcomputer. *

(No attempt at curve fitting has been made here, as the model is too simplified to be of interest other than as a means of demonstrating general behavior.) Curves A and D of fig. 2 and curves A of figs. 3 and 4 show that if one step is endothermic, the frequency spectrum may have a maximum. Such a maximum has been observed experimentally (fig. 2, inset). However, it is not possible to distinguish a fast endothermic step from a slow one, and the location of the peak is not simply related to the rate constant. This is exemplified by comparing curves A and D of fig. 2, as well as by taking into consideration that all curves in figs. 2–4 are unchanged on reversing the sign of the

---

* These results may readily be scaled to other values of the rate constants, since from eq. 14 it follows that, at any ω,

$$B(\omega) = \frac{r_1\left(r_2^2 + E_1^2\right)^{1/2}}{\left(r_1^2+1\right)^{1/2}\left(r_2^2+1\right)^{1/2}}$$

where $r_1 = k_1/\omega$ and $r_2 = k_2/\omega$.

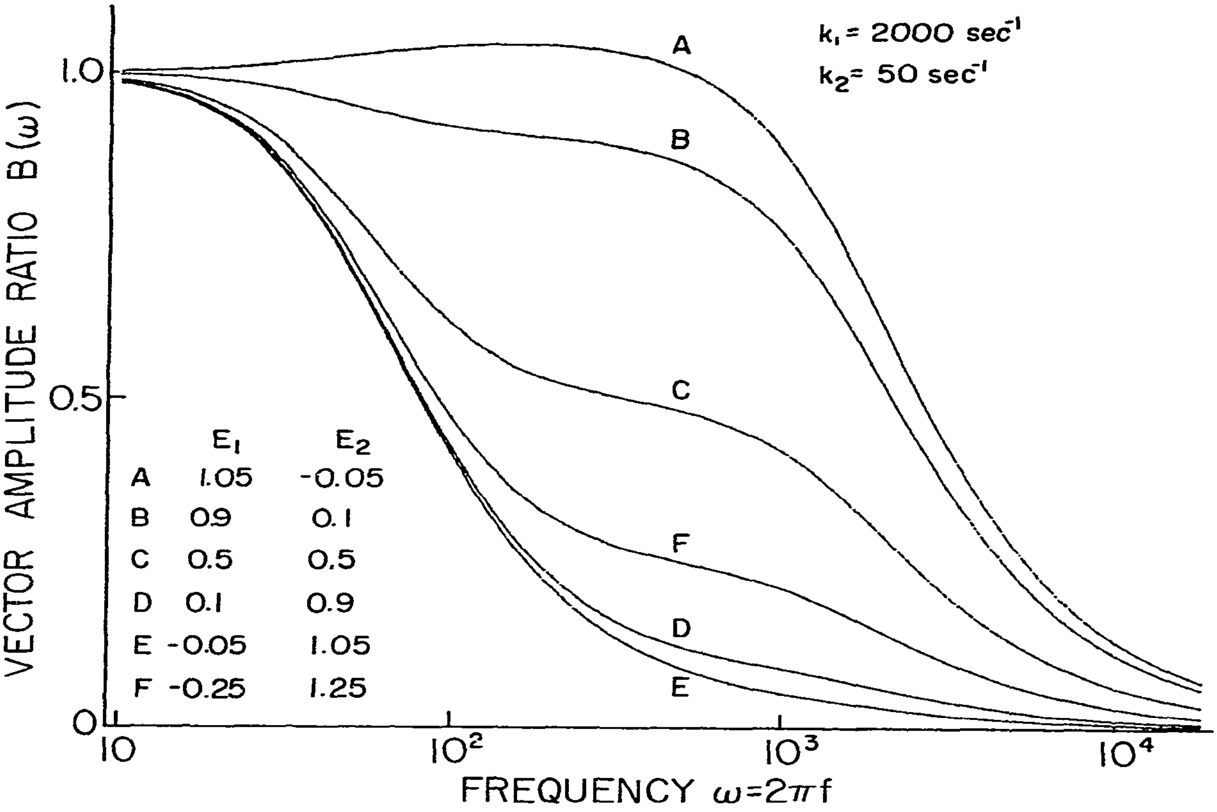

Fig. 4. Simulations of $B(\omega)$ for the model of fig. 1 with $k_1/k_2 = 40$. Curves E and F illustrate that fast endothermic transitions do not produce maxima unless they are large enough. It is seen that if the rate constants are sufficiently far apart, virtually complete resolution of the two transitions may be obtained (curve C).

value ascribed to E_1 and recalculating the value of E_2 from eq. 13. Increasing the ratio of the rate constants indefinitely does not alter the general character of curves such as A and D in fig. 1. If both steps are exothermic but close together the shape of the curves will change as E_1 and E_2 are varied, but unless the rate constants differ by an order of magnitude no discrete 'jumps' are seen with this model. Curves C of figs. 3 and 4 demonstrate that resolution becomes more pronounced as the ratio of the rate constants increases. Curves B and C of fig. 2 and B and D of figs. 3 and 4 show that if there are two exothermic steps, the step involving the greater dissipation of energy produces the largest (or sole) jump in $B(\omega)$; this occurs when the value of ω is in the vicinity of the corresponding rate constant. Relatively small differences in energetic parameters for the same rate constants are not easily distinguished as seen by a comparison of curves D and E of fig. 4.

These results suggest that by using photoacoustic magnitude frequency spectra alone it is possible to measure the gross kinetic features of a bioenergetic process, but not to determine a unique kinetic model for the enthalpy changes of the system. Net energy dissipated by the decay of several closely spaced intermediates may be measured. If a maximum is seen it is possible to assert that an endothermic step occurs (although the absence of a maximum cannot be taken as evidence for the nonoccurrence of an endothermic step); however, it is not possible to determine unambiguously at what time this step occurs.

4. Discussion and conclusions

Ort and Parson [10] measured the rapid enthalpy changes of suspensions of purple membrane fragments in buffer ($\text{pH} \approx 8.5$) at high and low ionic strengths excited with brief flashes of light, using a capacitor microphone calorimeter. Due to constraints of the system they were compelled to work at temperatures below 16 °C, most of the studies having been carried out between 2 and 14 °C. Under these conditions a drastic slowing down occurs, with the result that the time scale of the photocycle in their experiments appears to be of the order of 100 ms (rather than the usual 10 ms found at room temperature) [11]. Moreover, it is well known that at temperatures close to freezing-point, the O intermediate of the photocycle virtually disappears. The enthalpy changes, which are calculated from the temperature dependence of the volume changes observed, are essentially resolved into three phases following the 'immediate' storage of energy (i.e, 100 μs or less after the flash, when the enthalpy is found to be approx. 20 kcal/mol bR greater than before excitation): (a) fast release (fast expansion, ≈ 0.4 ms) of about 10 kcal/mol bR, loosely associated with proton release; (b) slow release (slow expansion, 12–20 ms) of about 40–45 kcal/mol bR, leaving the system with a deficit of about 35 kcal/mol bR as compared with before the flash; (c) relaxation to the original state (slow contraction, ≈ 80 ms) loosely associated with proton rebinding. An endothermic process is inferred to take place during phase c, and since relaxation to the original state is spontaneous the heat released in phase b must have been accompanied by an entropy decrease of at least 125 entropy units. As they point out, this implies a substantial increase in molecular order.

Garty et al. [3] reported comparable behavior in purple membrane suspensions at low ionic strength (pH 7.0 and 9.9), calculated from their photoacoustic frequency spectra. In their study, which was carried out at room temperature (19–22 °C), an additional exothermic step is resolved, and the endothermic step is seen directly as shown in the inset to fig. 2. Again, three principal phases could be distinguished after excitation and initial vibrational relaxation: (a) fast release ($\leqslant 0.3$ ms) of about 20 kcal/mol bR; (b) slow release (≈ 3.5 ms) of about 40 kcal/mol bR, leaving the system with a deficit of about 17 kcal/mol bR; (c) relaxation to original state ($\geqslant 5$ ms). In this case the heat released in phase b would have been accompanied by an entropy decrease of at least 57 entropy units, which still implies a considerable increase in molecular order.

To the extent that the model presented above is applicable, the results of Garty et al. may be interpreted in terms of the relative enthalpy changes E_1 and E_2, where $E_1 = (-40)/(-23) = 1.7$, $E_2 = 17/(-23) = -0.7$. However, as we have seen, the same magnitude frequency spectrum, in the absence of detailed knowledge of the phase relationships, accommodates the second possibility $E_1 = -1.7$, $E_2 = 2.7$. This represents an endothermic step of 40 kcal/mol bR preceding an exothermic step of 63 kcal/mol bR, with no deficit appearing. Since the endothermic step is spontaneous, the heat uptake would have been accompanied, if this is the case, by an entropy increase of at least 137 entropy units, i.e., a very marked increase in molecular disorder.

There are several lines of evidence to indicate that the second interpretation is more likely to be correct, i.e., that the photocycle involves a disordering followed by an ordering process, rather than the reverse. It should be noted that the results of Garty et al. do not permit any resolution of the issue, since by circumventing the problem of phase shift determination, information is lost. (The dimensions of this 'photoacoustic phase problem' were not appreciated at the time.) An order-disorder sequence, as claimed by Ort and Parson, and assumed by Garty et al., is certainly conceivable, for example, one would expect it if proton pumping involved the cyclic appearance and disappearance of a proton channel (we are indebted to Dr. Roberto Bogomolni for this suggestion). On the other hand, Cooper and Converse [12] used direct photocalorimetry to measure the transitional enthalpy changes in the related system bovine rhodopsin, and found the conversion of metarhodopsin I to metarhodopsin II to be an endothermic process. Sherman and Caplan [13] measured the relaxation of linear dichroism in bR phototransient (M band) absorption and showed the presence, despite the crystallinity of purple membrane, of chromophore rotational freedom, i.e., internal mobility within the molecule. Ahl and Cone [14] considerably extended these measurements and concluded that both photocycling and noncycling chromophores become rotationally displaced during the photocycle by up to 30° from their original positions, possibly as a result of rotations of entire bR molecules relative to each other. Frankel and Forsyth [15] carried out time-resolved X-ray diffraction studies of purple membrane, and observed major, reversible lattice alterations 1 ms and longer after light stimulation. All of these observations are consistent with a molecular disorder-order sequence of events.

Sturtevant [16] has identified the possible sources of the large heat capacity and entropy changes frequently observed in processes involving proteins. Of greatest importance are the conformational, hydrophobic, and vibrational effects, while the degree of exposure of charged groups to the aqueous environment and changes in hydrogen bonding may also give rise to significant contributions. All of these sources may be operative during the bR photocycle. Apart from conformational changes, there is evidence that both masking and exposure of polar groups occur; if this effect is a result of vertical displacement of the protein in the membrane as suggested by Eisenbach et al. [17], masking and exposure of nonpolar groups will tend to occur simultaneously. A net decrease in the exposure of both nonpolar groups and electrostatic charges should give rise to an increase in the entropy of the system [16]. A major factor, however, may well be charge displacements, particularly proton displacements. It is readily shown that transmembrane electrical potential differences in a suspension of fragments relax much faster than the events observed here, but diffusional relaxation is considerably slower and local concentration differences may persist. Charge displacements on a time scale of milliseconds have been observed, for example, by Slifkin et al. [18] and Rayfield [19].

Since the completion of the simulations discussed above a parallel study has appeared by Renard et al. [20]. In contrast to our work, these authors have simulated the in-phase component of the photoacoustic signal for a branched model of the bR photocycle, and curve-fitted their own in-phase frequency spectra. They also report magnitude frequency spectra. The model used assumes the presence of two M intermediates, one of which decays directly to the initial state while the other is associated kinetically with the O transient as originally suggested by Slifkin and Caplan [21] on the basis of modulation excitation spectroscopy. A parameter α evaluates the equilibrium between the two forms of M: if $\alpha = 1$ the branching disappears and the model becomes identical to that of fig. 1 with B identified as M and C as O. No simulations were performed for the case of an endothermic transition, since the data appeared not to indicate such a transition (although under certain conditions an indication was indeed found in the magnitude frequency spectra at the highest frequencies measured, ie., around 200 Hz, as was also found be LeGrange et al. [9]). The experimental in-phase signal was normalized using a photoinactive reference sample as in our studies. However, as we have seen in section 2, establishing a ratio between the sine components of the photoactive and photoinactive samples is not allowed because of differences in the phase shifts (unless the assumptions discussed are indeed shown to be valid). The magnitude frequency spectra, as the authors point out, are very similar to those of Garty et al. at frequencies above 70 Hz, but they did not detect an endothermic transition in the low-frequency region of the spectrum under any of the conditions tested. LeGrange et al. also obtained spectra resembling those of Renard et al. at low frequencies. The reason for the apparent disagreement between the various sets of data is not clear at present and will be investigated further. All are consistent with the occurrence of an early endothermic transition under favorable circumstances. The discrepancies undoubtedly have to do with differences in the preparations used.

Acknowledgements

This work was supported in part by a grant from the Kernforschungsanlage, Jülich, F.R.G., through the Israel National Council for Research and Development. We thank Drs. W. Stoeckenius, R.A. Bogomolni, and I.Z. Steinberg for illuminating discussions.

References

1 A. Rosencwaig and A. Gersho, J. Appl. Phys. 47 (1976) 64.
2 S. Malkin and D. Cahen, Photochem. Photobiol. 29 (1979) 803.
3 H. Garty, S.R. Caplan and D. Cahen, Biophys. J. 37 (1982) 405.
4 W. Stoeckenius, R. Lozier and R. Bogomolni, Biochim. Biophys. Acta 505 (1979) 215.
5 A. Danon and W. Stoeckenius, Proc. Natl. Acad. Sci. USA 71 (1974) 1234.
6 A. Warshel, Photochem. Photobiol. 30 (1979) 285.
7 B. Honig, T. Ebrey, R.H. Callender, U. Dinur and M. Ottolenghi, Proc. Natl. Acad. Sci. USA 76 (1979) 2503.
8 D. Oesterhelt and W. Stoeckenius, Nature 233 (1971) 149.
9 J. LeGrange, D. Cahen and S.R. Caplan, Biophys. J. 37 (1982) 4.
10 D.R. Ort and W.W. Parson, Biophys. J. 25 (1979) 355.
11 D.R. Ort and W.W. Parson, J. Biol. Chem. 253 (1978) 6158.
12 A. Cooper and C.A. Converse, Biochemistry 15 (1976) 2970.
13 W.V. Sherman and S.R. Caplan, Nature 265 (1977) 273.
14 P. Ahl and R. Cone, Biophys. J. 37 (1982) 229a.
15 R.D. Frankel and J.M. Forsyth, Biophys. J. 41 (1983) 15a.'
16 J.M. Sturtevant, Proc. Natl. Acad. Sci. USA 74 (1977) 2236.
17 M. Eisenbach, H. Garty, E.P. Bakker, G. Klemperer, H. Rottenberg and S.R. Caplan, Biochemistry 17 (1978) 4691.
18 M.A. Slifkin, H. Garty, W.V. Sherman, M.F.P. Vincent and S.R. Caplan, Biophys. Struct. Mech. 5 (1979) 313.
19 G.W. Rayfield, Biophys. J. 41 (1983) 109.
20 M. Renard, P. Thirion and M. Delmelle, Biophys. J. 44 (1983) 211.
21 M.A. Slifkin and S.R. Caplan, Nature 253 (1975) 56.